

In vivo total retinal blood flow measurement by Fourier domain Doppler optical coherence tomography

Yimin Wang

University of Southern California
Doheny Eye Institute and Department of Ophthalmology
Keck School of Medicine
1355 San Pablo Street, DVRC 160B
Los Angeles, California 90033

Bradley A. Bower

Joseph A. Izatt

Duke University
Department of Biomedical Engineering
136 Hudson Hall
Box 90281, Campus
Durham, North Carolina 27708

Ou Tan

David Huang

University of Southern California
Doheny Eye Institute and Department of Ophthalmology
Keck School of Medicine
1355 San Pablo Street, DVRC 160B
Los Angeles, California 90033

Abstract. There is considerable interest in new methods for the assessment of retinal blood flow for the diagnosis of eye diseases. We present *in vivo* normal human volumetric retinal flow measurement using Fourier domain Doppler optical coherence tomography. We used a dual-plane scanning pattern to determine the angle between the blood flow and the scanning beam in order to measure total flow velocity. Volumetric flow in each blood vessel around the optic nerve head was integrated in one cardiac cycle in each measurement. Measurements were performed in the right eye of one human subject. The measured venous flow velocity ranged from 16.26 mm/s to 29.7 mm/s. The arterial flow velocity ranged from 38.35 mm/s to 51.13 mm/s. The total retinal venous and arterial flow both added up to approximately 54 $\mu\text{l}/\text{min}$. We believe this is the first demonstration of total retinal blood flow measurement using the OCT technique. © 2007 Society of Photo-Optical Instrumentation Engineers. [DOI: 10.1117/1.2772871]

Keywords: optical coherence tomography; imaging; blood flow.

Paper 06309SSRR received Oct. 31, 2006; revised manuscript received Mar. 2, 2007; accepted for publication Mar. 9, 2007; published online Aug. 21, 2007.

1 Introduction

A comprehensive examination of ocular perfusion is needed to determine a patient's ocular hemodynamic status. A number of hemodynamic measurement techniques have been developed to assess various aspects of blood flow in the retina, in the choroids, and in the vessels that supply each.¹⁻⁶ One of these techniques, the pulsatile ocular blood flow (POBF),¹ is a pneumotonometer that uses a pressurized tip placed in contact with the cornea to measure intraocular pressure in real time. But the accuracy of this technique is limited because it gives an indirect measurement of blood flow. Through recording the movement of the retinal surface during fundus pulses throughout the cardiac cycle,² the retinal flow can be estimated. Fluorescein angiography^{3,4} can be used to visualize retinal hemodynamics, but the technique requires pupil dilation and dye injection. Furthermore, it is currently impossible to measure volumetric blood flow using angiography. The laser Doppler flowmeter (LDF) was developed to measure the volumetric blood flow in absolute units.^{5,6} But its accuracy is limited due to the lack of information about the speed distribution across the blood vessel and accurate vessel size. The inability to depth-resolve superimposed vessels is also one of the drawbacks of LDF.

Optical coherence tomography (OCT)⁷ is a noninvasive technology that is currently used for *in vivo* high-resolution sectional imaging of microstructure in biological tissues. By measuring singly backscattered light as a function of depth, OCT provides high-resolution, high-sensitivity *in vivo* images

of tissue structure. In addition to supplying morphological structure data on tissues, functional OCT techniques are also used to detect the birefringence⁸ and flow information⁹⁻¹² in biological tissue. But the application of Doppler OCT for retinal flow measurement was limited because of the low sampling rate in time domain OCT.¹³ The imaging speed of OCT has improved greatly with the development of the Fourier domain (FD) technique,^{14,15} making it possible to use OCT for *in vivo* blood flow measurement. The detection of ocular vessel pulsation with FD Doppler OCT has been reported.¹⁴ However, the FD Doppler OCT in this case was used only to measure flow speed in the direction of the scanning beam. The lack of speed information in the direction perpendicular to the scanning beam prevents a true measurement of flow speed. Although there are reports to measure the flow component perpendicular to the scanning beam by using velocity variance methods,¹⁶ the application of this method for retina flow measurement has not been reported. Currently, the reported Doppler OCT result is only for the speed measurement (mm/s), not volumetric flow (ml/min, or $\mu\text{l}/\text{min}$). In this paper, we report the development of FD Doppler OCT for *in vivo* retinal volumetric flow measurement. Our result shows that FD Doppler OCT can be used for the absolute measurement of the retinal volumetric flow without making any assumptions about anatomic and flow parameters.

2 Basic Principle

Optical Doppler OCT is based on the principle that moving particles, such as red blood cells inside a blood vessel, cause

Address all correspondence to Yimin Wang, Ph.D., Doheny Eye Institute—DVRC 160B, 1355 San Pablo Street, Los Angeles, CA 90033; Tel: 323-442-6746; Fax: 323-442-6688; E-mail: yiminwan@usc.edu

a Doppler frequency shift (Δf) to the light scattered according to

$$\Delta f = \frac{1}{2\pi}(\mathbf{k}_s - \mathbf{k}_i) \cdot \mathbf{V}, \quad (1)$$

where \mathbf{k}_i and \mathbf{k}_s are wave vectors of scanning and scattered light, respectively, and \mathbf{V} is the velocity vector of the moving particles. In an OCT system, only backscattered light is detected. Given the angle θ between the scanning beam and the flow direction, the Doppler shift is simplified to

$$\Delta f = -2Vn \cos \theta / \lambda_0, \quad (2)$$

where λ_0 is the center wavelength of the light source, and n is the refractive index of the medium. In FD-OCT, this frequency shift Δf will introduce a phase shift $\Delta\Phi$ in the spectral interference pattern that is captured by the line camera. With the fast Fourier transform (FFT), the transform result is a complex function characterized by amplitude and phase. Structure information can be obtained via the amplitude result. The phase difference between sequential axial scans at each pixel is calculated to determine the Doppler shift.^{14,17} Therefore, in addition to structural imaging, FD-OCT can be used to quantify blood flow parameters.

One limitation of phase-resolved flow measurement is an aliasing phenomenon caused by 2π ambiguity in the arctangent function. This phenomenon limits the maximum determinable Doppler shift to $\Delta f = 1/(2\tau)$, where τ is the time difference between sequential axial lines. Thus, the maximum detectable speed is $V = \lambda_0 / (4n\tau \cos \theta)$. From the expression, it can be seen that a short integration time τ can increase the maximum detectable speed. In practice, the maximum accessible Doppler frequency is limited by the detection speed of the line camera. The minimum detectable flow velocity is determined by the phase noise of the FD-OCT system.

Considering the cardiac cycles, the speed of the blood flow can be expressed as

$$V(x_v, z_v, t) = A(x_v, z_v)P(t), \quad (3)$$

where $A(x_v, z_v)$ is the speed distribution in the cross section of the blood vessel, and $P(t)$ shows the pulsation of the flow. With speed expression (3), the volumetric flow F can be calculated according to

$$\bar{F} = \int \int A(x_v, z_v) dx_v dz_v \cdot \frac{1}{T} \int_0^T P(t) dt, \quad (4)$$

where T is the period of pulsation. If flow speed $V(x_v, z_v, t)$ can be measured, the volumetric flow can be determined. However, from Eqs. (1) and (2), it can be seen that, in Doppler OCT, the frequency shift is caused by flowing particles with a velocity component in the direction of the illuminating beam. Doppler OCT only measures the value of $V \cos \theta$. To determine real flow speed V , the angle θ must be decoupled from the measured Doppler frequency shift. Therefore, more measurements are needed to determine angle θ .

Figure 1(a) shows the sampling beam scanning across the blood vessel twice with a displacement between two scanning planes S_1 and S_2 . A small step Δy_0 is chosen so that the blood

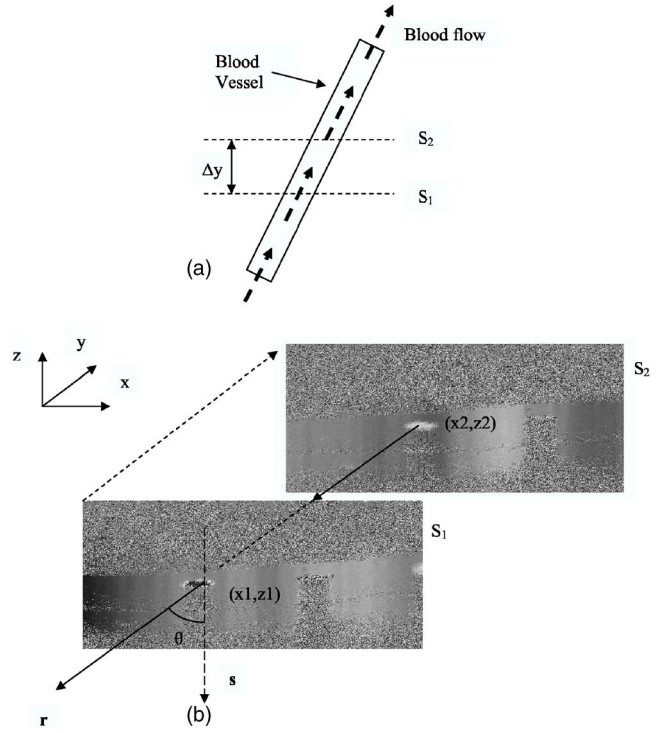


Fig. 1 (a) OCT beams scanning across the blood vessel with a displacement Δy . (b) Three-dimensional diagram of the scanning pattern shown in (a).

vessel between those two scanning planes has a linear shape. At the same time, because the step Δy_0 is small, the two scanning planes S_1 and S_2 are parallel to each other. In the coordinate system, if the OCT scan plane is defined as the x - and z -plane, then the y -axis would be the direction of the displacement. Figure 1(b) shows the three-dimensional diagram of the scanning pattern in Fig. 1(a). With displacement, the center of the blood vessel in those two scan planes can be computed as (x_1, z_1) and (x_2, z_2) separately. Therefore, in the coordinate system shown in Fig. 1(b), the vector of the blood vessel can be determined as $\mathbf{r}(\Delta x = x_1 - x_2, \Delta y = -\Delta y_0, \Delta z = z_1 - z_2)$. In the scanning plane, the scanning beam is always in the $-z$ -direction. So the vector of the scanning beam is $\mathbf{s}(0, 0, -1)$. With these two vectors, \mathbf{r} and \mathbf{s} , the angle θ between the scanning beam and the blood vessel can be determined as

$$\cos \theta = (\mathbf{r} \cdot \mathbf{s}) / R,$$

$$R = \sqrt{\Delta x^2 + \Delta y^2 + \Delta z^2}, \quad (5)$$

where R is the length of the vessel vector \mathbf{r} . From Eq. (5), the scanning angle θ can be determined as

$$\cos \theta = -\Delta z / R. \quad (6)$$

After the angle between the scanning beam and the blood vessel is determined, the flow direction can be identified through the sign of the frequency shift. This is explained in Fig. 2, in which the two flows in the same vessel with different flow directions in (a) and (b) will introduce different fre-

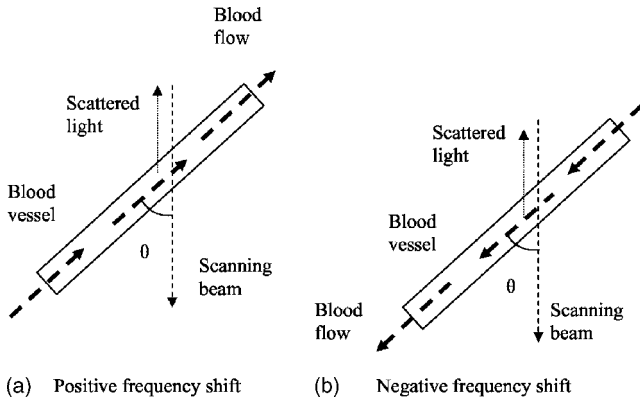


Fig. 2 When OCT beams scan through blood vessels, different flow directions lead to different frequency shifts.

quency shifts to the scattered beam. The left has a positive frequency shift and the right has a negative frequency shift. Therefore, with the measured frequency shift and the vector of the blood vessel, the flow direction can be determined. The information about flow direction will help us to separate the arteries from veins for the vessels distributed around the optic disc, because arteries have a flow direction into the retina from the nerve head, and veins have a flow direction toward the nerve head from the retina.

To calculate the volumetric blood flow, the integration in Eq. (4) should be calculated in the plane P_v , which is normal to the blood vessel (flow) direction, as shown in Fig. 3(b). But in practice, the OCT plane S_0 is not perpendicular to the flow direction, or we would have no Doppler signal, as shown in Fig. 3(b). If the angle β between the planes P_v and S_0 can be determined, the flow equation (4) can be rewritten as

$$\bar{F} = \iint A(x, z) \cos \beta dx dz \cdot \frac{1}{T} \int_0^T P(t) dt. \quad (7)$$

It can be seen that with the introduction of angle β , the integration can be done in the OCT plane. According to the geometrics, the angle between two planes can be calculated by two vectors, which are normal to them separately. For P_v , the vector perpendicular to it is \mathbf{r} , as shown in Fig. 3(a). For the OCT plane S_0 , because it is an x, z -plane, the vector perpendicular to it is the y -axis, $(0, 1, 0)$. Thus, the angle β between P_v and S_0 is

$$\cos \beta = (\mathbf{r} \cdot \mathbf{y})/R = \Delta y_0/R. \quad (8)$$

3 Experimental Setup

The Fourier domain OCT (FD-OCT) system is shown in Fig. 4. It contains a superluminescent diode with a center wavelength of 841 nm and a bandwidth of 49 nm. The axial resolution, as defined by the source bandwidth, is 6.4 μm in air. The measured axial resolution was 7.5 μm in air. The deviation from theoretical value is due to the non-Gaussian spectrum profile. Considering the refractive index of tissue, the axial resolution would be 5.36 μm in tissue. The beam spot size was about 1.3 mm onto the cornea. The transverse resolution is about 20 μm , as limited by the optics of the eye.

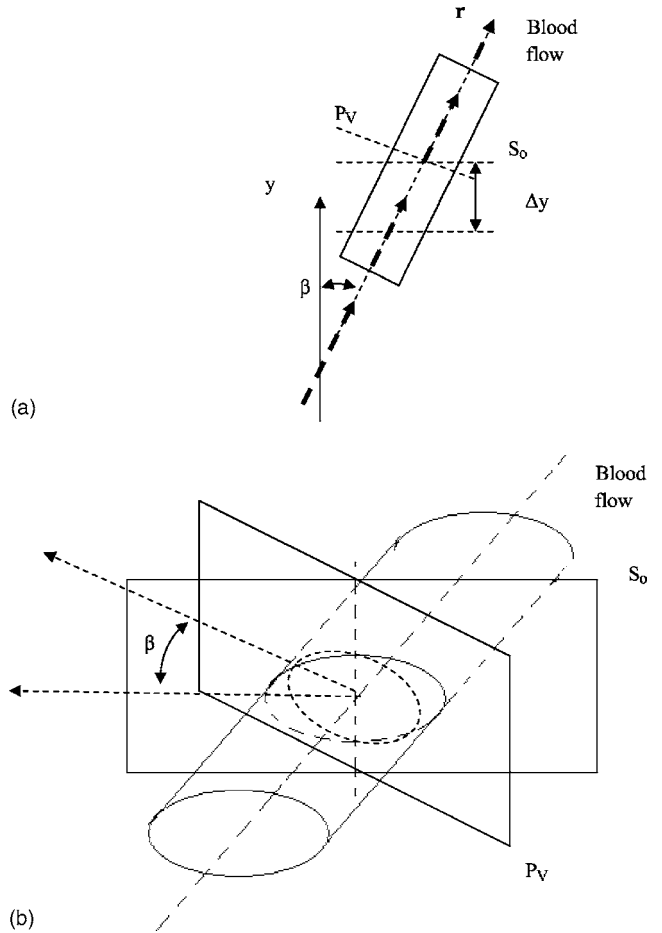


Fig. 3 (a) The angle β between the OCT plane S_0 and the plane normal to the flow direction P_v ; (b) the relationship between P_v and S_0 in 3D diagram.

Light from the source travels through an 80/20 coupler with 80% of the source power entering the reference arm of a standard Michelson interferometer and 20% entering the sample arm. The reference arm consists of an objective that focuses light through a 1-in. dispersion-matching water cell and a neutral density filter to a silvered mirror. The sample arm contains a standard slit-lamp biomicroscope base that has been adapted with custom OCT scanning optics. Power incident on the cornea is 500 μW , which is well below the ANSI limits for extended beam exposure. Reference and sample arm light interfere in the fiber coupler, and the composite signal is detected by a custom spectrometer. The spectrometer contains a 1024-pixel line-scan camera. Data from the camera are transferred via the Cameralink interface to a high-end PC. The data consist of 512 (axial) \times 1000 (transverse) image lines, which are acquired, processed, streamed, and displayed at 17 frames per second using custom acquisition software provided by BiopTigen, Inc. (Durham, NC). This imaging rate allows for fast volume acquisition. The theoretical signal-to-noise ratio for this system is 110 dB given at 100- μs integration time, while the measured SNR was 107 dB at 200 μm from the zero-path length difference location. With $\lambda_0=841$ nm, the time interval between two sequential A lines $\tau=56$ μs (in which integration time is 50 μs , and the data transfer time is

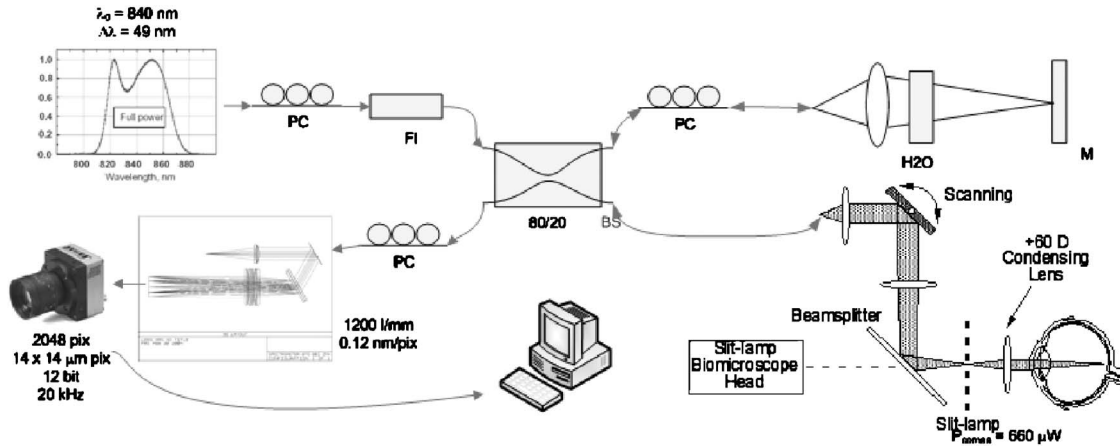


Fig. 4 The Fourier domain OCT retinal imaging system.

6 μ s), the maximum determinable Doppler shift is 8.9 KHz, and the maximum detectable speed in the eye ($n=1.33$) is 2.8 mm/s without considering the influence of angle θ . The measured minimum detectable Doppler frequency shift is 51 Hz according to phase noise, and the minimum determinable speed is 16.3 μ m/s.

4 Flow Measurement

The distribution of blood vessels around the optic nerve head in the right eye of a volunteer subject was recorded *in vivo* by three-dimensional OCT scanning (scanning area was 5 mm \times 5 mm), as shown in Fig. 5, which we got when we saw the 3D image from the top (nerve head side). Seventeen vessels can be identified around the nerve head in this measurement; these are labeled from 1 through 17.

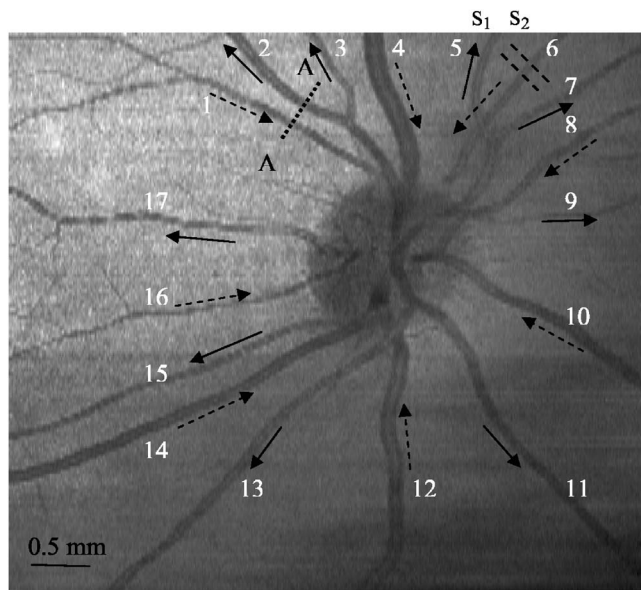
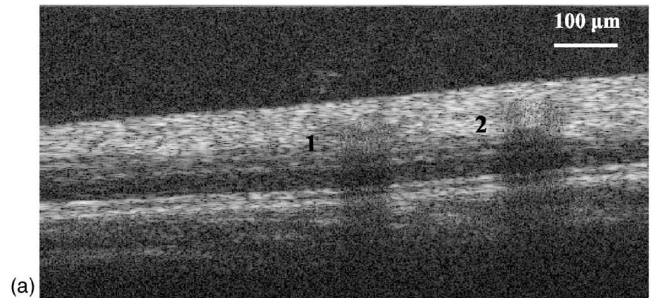
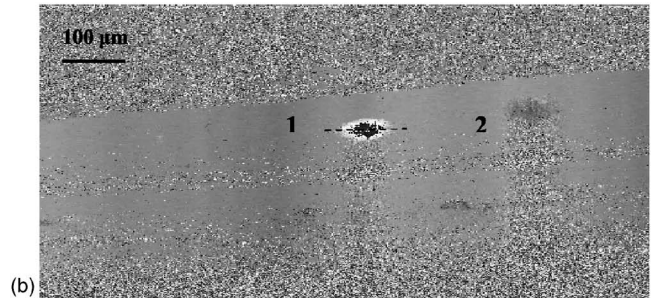


Fig. 5 Fundus image recorded by three-dimensional OCT scan. The vessels around the nerve head are labeled from 1 to 17. The solid and dashed arrows show the flow direction for each vessel.

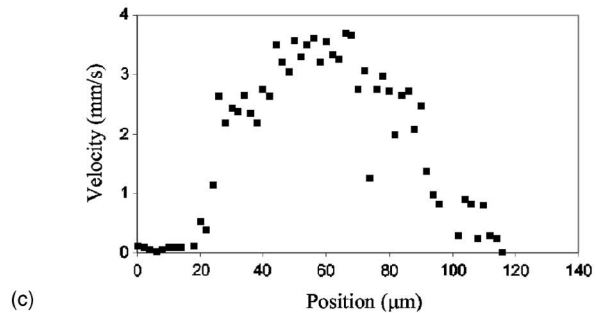
Figure 6 shows the OCT and Doppler OCT images recorded by our FD-OCT system (image size is 1.0 \times 1.07 mm). The scanning position is shown in Fig. 5 as dashed line AA across vessels 1 and 2. The OCT structure



(a)



(b)



(c)

Fig. 6 (a) OCT structure image; (b) Doppler frequency shift image; (c) speed profile for the position marked as dashed line in (b).

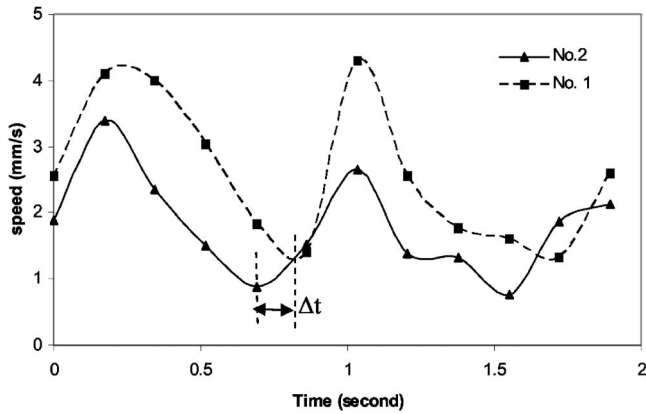


Fig. 7 Flow speed variation with time for the vessels shown in Fig. 6. The dashed curve is for vessel 1, and the solid curve is for vessel 2.

image is shown as Fig. 6(a). Figure 6(b) shows the Doppler frequency image. Two vessels can be identified in Fig. 6(b). Vessel 1 has a positive frequency shift. The black part in the center of vessel 1 is due to the phase wrapping. After phase unwrapping¹⁸ and subtracting the influence of background motion,¹⁴ the flow distribution can be recovered. Figure 6(c) shows the speed profile of the blood flow marked as the

dashed line in vessel 1. In Fig. 6(b), the right flow signal is from vessel 2, which has a negative frequency shift.

Using continuous scanning of the blood vessel, the Doppler signals were recorded at different times. The flow speed at the center part of the two vessels shown in Fig. 6(b) was analyzed. Figure 7 shows the variation of peak flow speed at different times. The dashed curve is for vessel 1, and the solid curve with triangle symbols is from vessel 2. These two curves show a pulsation rate of 70 beats/min, equal to the heart rate of the volunteer. The speed curve of vessel 1 shows a time delay of Δt in the pulsation compared with that of vessel 2, indicating that these are different types of vessels. The pulsation of vessel 2 occurs earlier than that of vessel 1, indicating that it is an artery. Vessel 1 should be a vein.

To measure the angle between the input beam and the blood vessel, the OCT scanning beam is scanned at two positions, S_1 and S_2 , with a step of 0.2 mm along the vessel for several seconds, as shown by the double dashed lines across vessel 6 in Fig. 5. The flow pulsation can be detected in this period. The flow signal in Fig. 8(a) shows the measured Doppler frequency shift from blood vessel 6. It has a negative frequency shift with positive phase wrapping at the center. After phase unwrapping, the flow profile $A(x, z)$ can be determined, as shown in Fig. 8(c). Figure 8(b) shows the 2D frequency shift distribution before phase unwrapping. The mea-

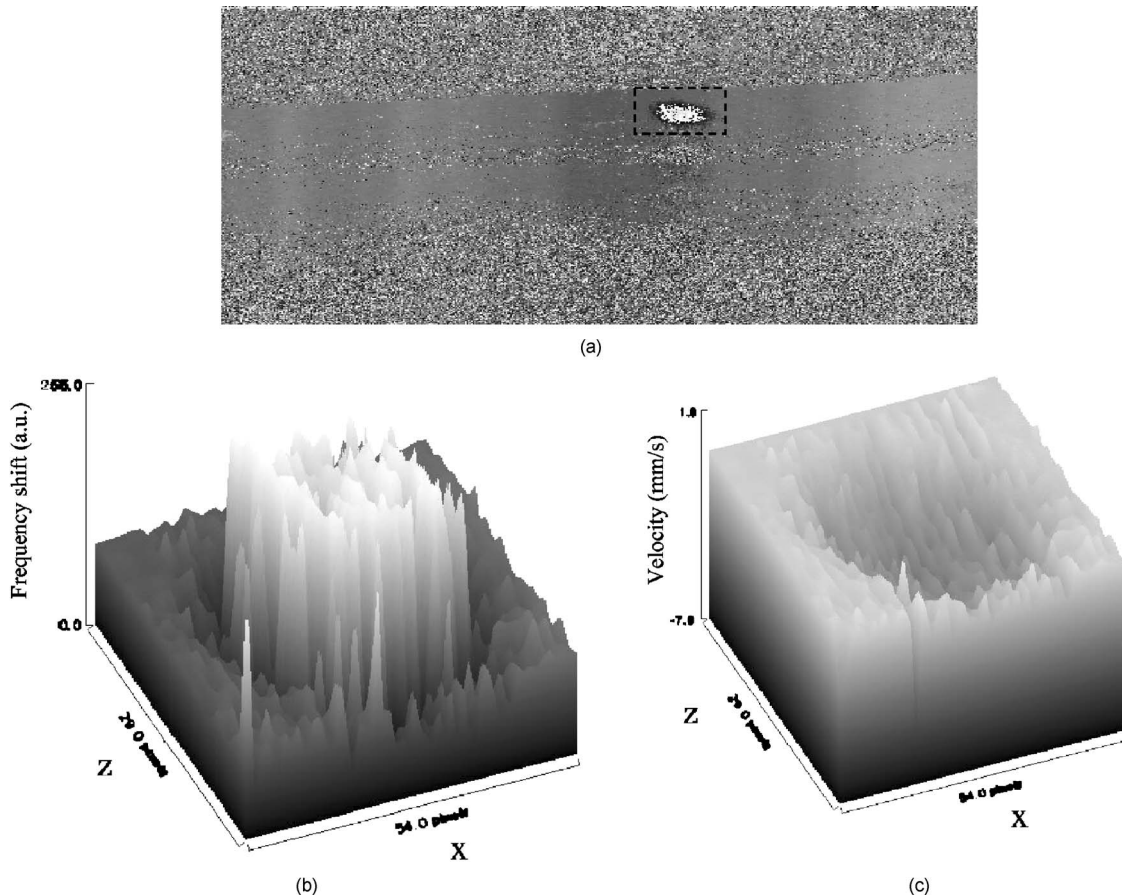


Fig. 8 Two-dimensional speed distribution. (a) Doppler frequency shift image for vessel 6; (b) three-dimensional speed distribution for the vessel marked by the dashed line in (a); (c) speed distribution after phase unwrapping.

Table 1 Diameter, flow speed, and flow volume for the retina veins.

Vessel Number	Diameter (μm)	Peak Velocity (mm/s)	Flow ($\mu\text{l}/\text{min}$)
1	72	16.62	2.52
4	150	28.57	15.75
6	78	21.89	3.18
8	68	23.01	4.65
10	88.8	24.59	5.62
12	114	29.7	11.01
14	114.7	27.0	10.21
16	44.4	21.88	1.77

sured position differences of vessel 6 at two sequential OCT images are $\Delta x=10 \mu\text{m}$ and $\Delta z=-31.45 \mu\text{m}$. Thus, the vector of the blood vessel is (10, -200, -31.45). From Eq. (6), the angle between the scanning beam and blood vessel can be calculated as $\cos \theta=0.16$, and $\theta=80.8^\circ$. With the value of $\cos \theta$, the calculated maximum flow speed in vessel 6 is 21.9 mm/s. From Eq. (8), the angle β can be calculated as $\cos \beta=0.99$. With these parameters, the volumetric flow in vessel 6 is calculated as 3.18 $\mu\text{l}/\text{min}$ with Eq. (7).

With the vector of vessel 6 and its negative frequency shift, the flow direction in vessel 6 can be identified according to the discussion of Fig. 2. It is from scanning plane S_2 to S_1 . In our scanning pattern in Fig. 5, plane S_1 is close to the nerve head compared with S_2 . Thus, this flow is toward the optic disc, and blood vessel 6 is a vein. For vessel 1, the measured peak speed was 16.62 mm/s. The calculated blood flow was 2.52 $\mu\text{l}/\text{min}$. The determined flow direction in vessel 1 is into the optic disk. It is a vein. For vessel 2, the measured peak flow speed was 49.17 mm/s. The calculated flow was 6.96 $\mu\text{l}/\text{min}$. The determined flow direction is from the disk to the retina. Thus, vessel 2 is an artery. This agrees with the distinction based on the time course for pulsatile flow velocity variation shown in Fig. 7, where the systolic peak and diastolic trough in flow velocity in the artery can be seen to slightly precede those in the vein.

The blood flow distribution around the optic disc was characterized by measuring each vessel individually. The flow direction is labeled in Fig. 5, where the solid arrow shows the blood flow direction to be from nerve head into the retina. Those vessels are arteries. The dashed arrows are for veins in which the blood flow is from the retina to the nerve head. The vessel size, peak flow velocity, and flow volume were calculated and shown in Tables 1 and 2 for veins and arteries, separately. It can be seen that arteries and veins can also be distinguished by their peak flow velocities. In this subject, roughly speaking, the maximum speeds are less than 30 mm/s in veins and greater than 38 mm/s in arteries. Summation of those flows gives the total flow out of the retina from veins as 54.71 $\mu\text{l}/\text{min}$.

Table 2 Diameter, flow speed, and flow volume for the retinal arteries.

Vessel Number	Diameter (μm)	Peak Velocity (mm/s)	Flow ($\mu\text{l}/\text{min}$)
2	77.7	49.17	6.96
3	51.8	45.11	3.23
5	62.9	43.61	6.95
7*	70.3	51.13	8.8
9*	33.3	78.2	2.49
11*	85.1	47.37	8.72
13*	74	38.35	7.52
15*	66.6	48.2	4.29
17*	70.3	48.57	4.93

5 Discussion

The results show that with dual-plane scanning pattern, the real flow speed can be determined. To calculate the flow volume according to Eq. (7), the pulsatile flow was measured and averaged over one cardiac cycle. For a few arteries, the systolic velocity caused signal fading. Fortunately, it was still possible to measure flow during diastole (minimum flow portion of the cardiac cycle). For these arteries, we estimated the average flow by the ratio k between the average flow speed and the minimum speed that could be calculated from other arteries that did not exceed the system dynamic range during the entire cardiac cycle. During continuous scanning, the minimum flow speed can be detected for an artery. Then the peak flow of the artery is estimated with the lowest speed multiplied by this factor k . The vessel in Table 2 shows the artery result. The arteries marked with * are estimated values. To detect the volumetric flow from arteries as accurately as from veins, the Doppler OCT system with high determinable range is needed. Because the diameter of vessel 9 was much smaller than other vessels, a high scanning density was employed to get a good speed profile for flow calculation. A high scanning density leads to a low frame rate. So the sampled smallest speed is not the real minimum flow speed in vessel 9. This leads to the overestimated speed value, which is higher than other arteries. Table 3(b) shows the statistical result for

Table 3 Statistical result for retinal flow measurement by FD-OCT.

	Artery	Vein
Maximum velocity (mm/s)	51.13	29.7
Minimum velocity (mm/s)	38.35	16.62
Total flow ($\mu\text{l}/\text{min}$)	53.89	54.71

this measurement. The total arterial flow was $53.89 \mu\text{l}/\text{min}$. This is close to the total venous flow of $54.71 \mu\text{l}/\text{min}$. In literature, the measured total arterial and venous flows were $33 \pm 9.6 \mu\text{l}/\text{min}$ and $34 \pm 6.3 \mu\text{l}/\text{min}$, respectively, by laser Doppler velocimetry.¹⁹ Our measurement result is comparable with these results. Because the total venous flow volume is identical to that of arteries in the retina, as shown by Riva and colleagues,¹⁸ the total venous flow can be used to quantify the retinal blood flow. The limited velocity range that can be measured with our OCT system only affects arterial measurements. We can still fully assess retinal blood flow by limiting our measurements to the veins.

Accurate quantification of ocular blood flow is of increasing importance in studying glaucoma. Although other measurement techniques have been developed to assess various aspects of blood flow in the retina and choroids,^{1-3,5} different assumptions are needed for those techniques to quantify the flow. For example, POBF requires several assumptions about scleral rigidity, and a universal intraocular pressure eye volume relationship is needed. Moreover, most of these techniques do not produce direct and absolute flow measurements, but employ with arbitrary units that only indirectly reflect on flow. In coherence flow measurement,² it detects the interference pattern formed by the laser light partially reflected by both the cornea and the retina to determine the fundus movement in micrometers. This movement is used as a surrogate for choroidal blood flow.

The LDF velocity measurement is based on the Doppler principle, wherein the light reflected by moving blood cells is Doppler-shifted and returns with a slightly altered frequency. The velocity can be determined by analyzing this frequency shift. Because information about the speed distribution across the vessel is lacking, the flow volume calculation requires an assumed relationship between the maximum Doppler shift and the true average blood velocity. A photographic measurement of vessel diameter is used to convert velocity to flow in LDF. Since the external diameter is more visible than the inner diameter of the blood vessel, this measurement may overestimate the cross-sectional flow area and the volumetric flow.

We describe the first retinal flow measurement method that produces absolute flow measurement over the cardiac cycle without resorting to any assumptions on anatomic or flow parameters. The measured result in volume flow units can be compared between different subjects. Because the current measurement is for one vessel at a time, this speed is slow for clinical applications. A fast scanning pattern will be developed for quick assessment of the retinal flow.

6 Summary

We present *in vivo* retinal flow measurement using Fourier domain Doppler optical coherence tomography. A dual-plane scanning pattern was used to determine the angle between the blood flow and scanning beam so that the total flow velocity can be measured. Based on their different flow directions, arteries can be distinguished from veins. Volumetric flow in each blood vessel around the optic nerve head was integrated in one cardiac cycle in each measurement. The total retinal venous flow was $54.71 \mu\text{l}/\text{min}$, and the total arterial flow

was $53.89 \mu\text{l}/\text{min}$. We believe this is the first demonstration of total blood flow measurement with OCT.

Some limitations of the technique were observed. Signal fading from excessive flow velocity occurred in some arteries during systole. Shortening signal integration time may extend the detectable velocity range. Individually measuring the flow in each retinal vessel proved tedious. A fast scanning method will be investigated to include multiple vessels, possibly all retinal vessels, in a single scan.

Acknowledgments

This work was supported by NIH Grants R01 EY013516 and P30 EY03040 and by a grant from Research to Prevent Blindness. Support from Bioptigen, Inc. is also gratefully acknowledged. Financial interest disclosures: David Huang receives patent royalties, a research grant from Carl Zeiss Meditec, Inc. and receives consulting fees (stock options) and a research grant from Optovue Inc. Joseph Izatt and Bradley Bower are part-time employees of Bioptigen, Inc. Yimin Wang and Ou Tan have no financial interest in the topic of the article.

References

1. M. E. Langham and K. F. To'mey, "A clinical procedure for the measurement of the ocular pulse-pressure relationship and the ophthalmic arterial pressure," *Exp. Eye Res.* **27**, 17–25 (1978).
2. A. F. Fercher, "In vivo measurement of fundus pulsations by laser interferometry," *IEEE J. Quantum Electron.* **QE-20**, 1469–1471 (1984).
3. R. W. Flower, "Extraction of choriocapillaris hemodynamic data from ICG fluorescence angiograms," *Invest. Ophthalmol. Visual Sci.* **34**, 2720–2729 (1993).
4. Y. Hirata, H. Nishiwaki, S. Miura, Y. Leki, Y. Honda, K. Yumikake, Y. Sugino, and Y. Okazaki, "Analysis of choriocapillaris flow patterns by continuous laser targeted angiography in monkeys," *Invest. Ophthalmol. Visual Sci.* **45**, 1954–1962 (2004).
5. C. Riva, B. Ross, and G. B. Benedek, "Laser Doppler measurements of blood flow in capillary tubes and retinal arteries," *Invest. Ophthalmol.* **11**, 936–944 (1972).
6. M. D. Stern, D. L. Lappe, P. D. Bowen, J. E. Chimosky, G. A. Holloway, Jr., H. R. Keiser, and R. L. Bowman, "Continuous measurement of tissue blood flow by laser Doppler spectroscopy," *Am. J. Physiol.* **232**, H441–H448 (1977).
7. D. Huang, E. A. Swanson, C. P. Lin, J. S. Schuman, W. G. Stinson, W. Chang, M. R. Hee, T. Flotte, K. Gregory, C. A. Puliafito, and J. G. Fujimoto, "Optical coherence tomography," *Science* **254**, 1178–1181 (1991).
8. J. F. de Boer, T. E. Milner, M. J. C. van Gemert, and J. S. Nelson, "Two-dimensional birefringence imaging in biological tissue by polarization-sensitive optical coherence tomography," *Opt. Lett.* **22**, 934–936 (1997).
9. X. J. Wang, T. E. Milner, and J. S. Nelson, "Characterization of fluid flow velocity by optical Doppler tomography," *Opt. Lett.* **20**, 1337–1339 (1995).
10. J. A. Izatt, M. D. Kulkarni, S. Yazdanfar, J. K. Barton, and A. J. Welch, "In vivo bidirectional color Doppler flow imaging of picoliter blood volumes using optical coherence tomography," *Opt. Lett.* **22**, 1439–1441 (1997).
11. Z. Chen, T. E. Milner, D. Dave, and J. S. Nelson, "Optical Doppler tomography imaging of fluid flow velocity in highly scattering media," *Opt. Lett.* **22**, 64–66 (1997).
12. Y. Zhao, Z. Chen, C. Saxer, S. Xiang, J. F. de Boer, and J. S. Nelson, "Phase resolved optical coherence tomography and optical Doppler tomography for imaging blood flow in human skin with fast scanning speed and high velocity sensitivity," *Opt. Lett.* **25**, 114–116 (2000).
13. S. Yazdanfar, A. M. Rollins, and J. A. Izatt, "In vivo imaging of human retinal flow dynamics by color Doppler optical coherence tomography," *Arch. Ophthalmol. (Chicago)* **121**, 235–239 (2003).

14. B. R. White, M. C. Pierce, N. Nassif, B. Cense, B. H. Park, G. J. Tearney, B. Bouma, T. C. Chen, and J. F. de Boer, "In vivo dynamic human retinal blood flow imaging using ultra-high-speed spectral domain optical Doppler tomography," *Opt. Express* **11**, 3490–3497 (2003).
15. M. Wojtkowski, V. J. Srinivasan, T. H. Ko, J. G. Fujimoto, A. Kowalczyk, and J. S. Duker, "Ultrahigh-resolution, high-speed, Fourier domain optical coherence tomography and methods for dispersion compensation," *Opt. Express* **12**, 2404–2422 (2004).
16. Y. Zhao, Z. Chen, C. Saxer, Q. Shen, S. Xiang, J. F. De Boer, and J. S. Nelson, "Doppler standard deviation imaging for clinical monitoring of *in vivo* human skin blood flow," *Opt. Lett.* **25**, 1358–1360 (2000).
17. R. A. Leitgeb, L. Schmetterer, C. K. Hitzenberger, A. F. Fercher, F. Berisha, M. Wojtkowski, and T. Bajraszewski, "Real-time measurement of *in vitro* flow by Fourier-domain color Doppler optical coherence tomography," *Opt. Lett.* **29**, 171–173 (2004).
18. D. C. Ghiglia, G. A. Mastin, and L. A. Romero, "Cellular-automata method for phase unwrapping," *J. Opt. Soc. Am. A* **4**, 267–280 (1987).
19. C. E. Riva, J. E. Grunwald, S. H. Sinclair, and B. L. Petrig, "Blood velocity and volumetric flow rate in human retinal vessels," *Invest. Ophthalmol. Visual Sci.* **26**, 1124–1132 (1985).